Article

Screening of Scaffolds for the Design of G-Quadruplex Ligands

Joana Figueiredo [1], David Peitinho [2], Maria Paula Cabral Campello [2], Maria Cristina Oliveira [2], António Paulo [2], Jean-Louis Mergny [3,4] and Carla Cruz [1,*]

[1] Centro de Investigação em Ciências da Saúde, Universidade da Beira Interior, Av. Infante D. Henrique, 6200-506 Covilhã, Portugal; figueiredo_joana@hotmail.com

[2] Centro de Ciências e Tecnologias Nucleares, Instituto Superior Técnico, Universidade de Lisboa, Estrada Nacional 10 (km 139.7), 2695-066 Bobadela, Portugal; dpeitinho@ctn.tecnico.ulisboa.pt (D.P.); pcampelo@ctn.tecnico.ulisboa.pt (M.P.C.C.); cristinaoliveira@ctn.tecnico.ulisboa.pt (M.C.O.); apaulo@ctn.tecnico.ulisboa.pt (A.P.)

[3] Institute of Biophysics of the CAS, v.v.i., Královopolská 135, 612 65 Brno, Czech Republic; jean-louis.mergny@polytechnique.edu

[4] Laboratoire d'Optique et Biosciences, Ecole Polytechnique, CNRS, INSERM, Institut Polytechnique de Paris, 91128 Palaiseau, France

* Correspondence: carlacruz@fcsaude.ubi.pt

Abstract: In the last decade, progress has been made in G-quadruplex (G4) ligands development, but for most compounds, the ligand binding mode is speculative or based on low resolution methods, with its discovery based on structure-based approaches. Herein, we report the synthesis of small (MW < 400 Da) heterocycle compounds, containing different aromatic scaffolds, such as phenyl, quinoline, naphthalene, phenanthroline and acridine moieties, in order to explore their stabilization effect towards different DNA G4s, such as those found in c-MYC, KRAS21 and VEGF promoters, 21G human telomeric motif and pre-MIR150. The fluorescence resonance energy transfer (FRET) melting assay indicates that the acridine moiety is the most active scaffold, followed by phenanthroline. The different scaffolds are promising in terms of drug-like properties and, in general, the IC50 values of the respective heterocycle compounds are lower in a cancer cell line, when compared with a normal cell line. The acridine derivative C_5NH_2 has the most favorable cytotoxic profile in terms of cell selectivity.

Keywords: G-quadruplex; heterocycle compounds; scaffolds; drug-design

1. Introduction

The formation of G4 requires monovalent (Na^+ and K^+) or divalent/multivalent (e.g., Sr^{2+}) cations, or small molecules, known as G4 ligands, which are chemical compounds that specifically bind and stabilize the structure of G4. Many efforts are being made to target G4s as a therapeutic approach, given their implication in carcinogenesis [1] or virology [2]. As such, G4s provide recognition sites for ligands, since different G4 structures adopt specific conformations. These ligands generally have an aromatic surface, allowing π–π stacking interactions with a terminal G-quartet, one or more positive charge(s) or basic groups to selectively bind to the loops or grooves of the G4, and a geometry/shape preventing intercalation into double-stranded DNA. Many G4 ligands have characteristic cores that can be chemically modified, allowing the synthesis of various analogues whose therapeutic activity in cancer is being investigated. Disubstituted amidoanthraquinones were the first G4 ligands to be reported [3]. Later on, the cationic porphyrin TMPyP4 emerged as a potent telomerase inhibitor upon binding to telomeric G4s [4]. However, TMPyP4 also binds to duplex and triplex DNA [5,6]. Natural compounds, such as telomestatin, berberine and its derivatives, were considered potent telomerase inhibitors [7,8]. However, the structural complexity of telomestatin is a huge obstacle for its efficient large-scale synthesis and production as a drug. Pyridostatin, BRACO-19, naphthalene diimides and bisquinolinium

compounds, such as PhenDC3, have been used to broadly promote G4 formation in high-throughput sequencing of G4 structures [9]. Some of these G4 ligands have entered clinical trials, namely the fluoroquinolones CX-3543 and CX-5461, that selectively bind and stabilize a broad spectrum of G4 structures, including those harboured in c-MYC, c-KIT, and telomeres [10]. These fluoroquinolones interact with a G4 found in ribosomal DNA and disrupt the binding between these G4s and protein complexes, thereby inhibiting ribosome biogenesis [11]. Other novel ligands were reported to be selective for a sub-class of quadruplex structures, such as the diquinolinyl-pyridine ligands, that show a preference for the parallel conformation of telomeric, c-MYC and c-KIT G4s [12], or ToxaP, which prefers an antiparallel fold [13].

However, there is still a long way to go for the development of G4 ligands. Indeed, the multiplicity of potential targets, the variety of ligand binding sites and the differences in the ligand effects, in vitro and in vivo, make it difficult to unravel if the stabilization or destabilization of G4s promotes or inhibits gene expression. A major limitation for the clinical application of G4 ligands is related to their selectivity and potential side effects on normal cells. In this regard, it is important to screen different scaffolds and analyze the binding to G4s and the cellular effects on normal cells and cancer cells. In this context, we synthetized and tested some heterocycle compounds that will be able to act as a scaffold for G4 ligand/drug design. Different scaffolds, such as quinoline, phenyl, acridine and phenanthroline (Figure 1), were investigated to their capacity to stabilize different DNA and RNA G4 structures by the FRET melting assay [14]. Additionally, the in silico molecular properties were predicted and the cytotoxicity effects were also evaluated in a lung cancer cell line (A549) vs. normal cell (NHDF).
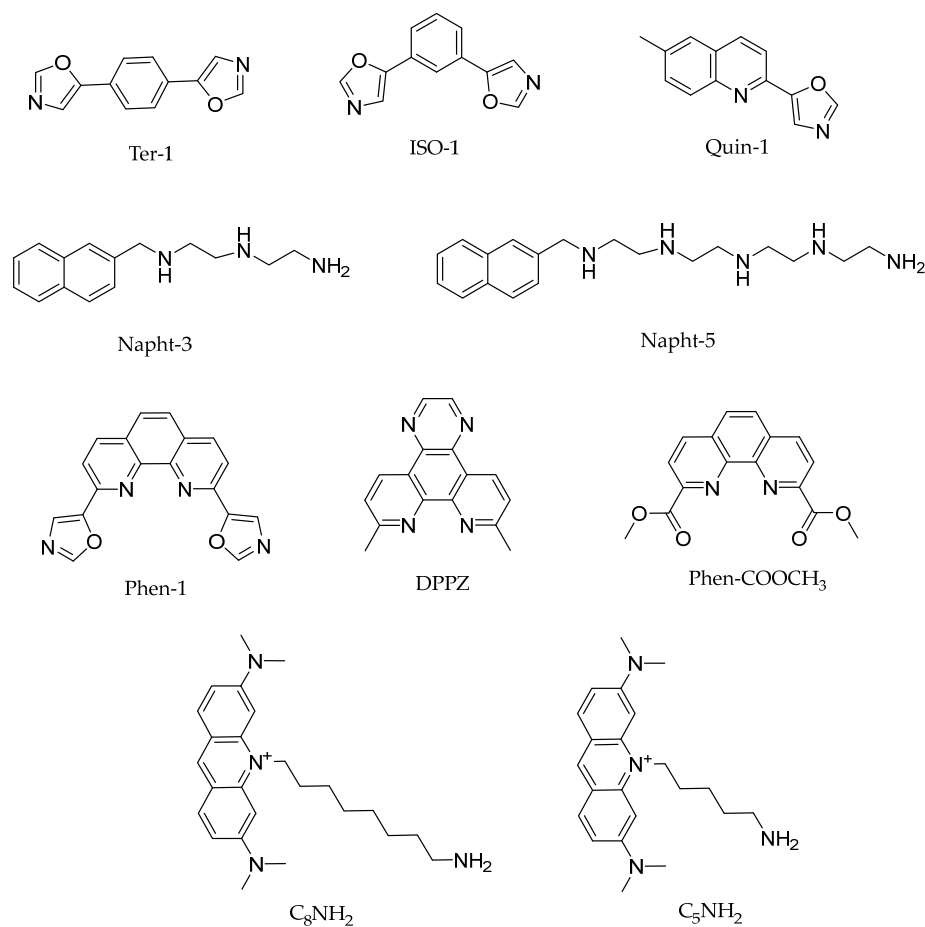

Figure 1. Chemical structures of the different scaffolds used in the study.

2. Materials and Methods

2.1. Chemical Synthesis

All reagents and solvents were used without additional purification, unless stated otherwise, and were obtained from commercial suppliers such as Sigma-Aldrich (St. Louis, MO, USA) and Across Organics (Geel, Belgium). Chemical reactions were followed by thin-layer chromatography (TLC) using Merck-Nagel (0.2 mm) plates which are visualized by UV detection. Melting points were measured for in vitro tested compounds and were recorded on a Büchi B-540 melting point apparatus and are uncorrected.

[1]H and ^{13}C spectra were performed at 25 °C on a Bruker Avance III 400 MHz spectrometer with a TXI probe. The spectra were processed in the software MestReNova 12.0.0. (Mestrelab Research S.L., Santiago de Compostela, Spain) and are presented in the Supplementary Material (Figure S1).

2.1.1. Synthesis of Phenyl and Quinoline Derivatives

The synthesis of 1,4-bis(oxazol-5-yl)benzene (Ter-1), 1,3-bis(oxazol-5-yl)benzene (ISO-1) and 6-methyl-(2-oxazol-5-yl)quinoline (Quin-1) was performed as previously described [15].

2.1.2. Synthesis of Naphthalene Derivatives

The naphthalene derivatives ligands were prepared according to methods described previously, with slight modifications [16]. Briefly, to a solution of the desired polyamine (1.0 g, 9.6 mmol) in a mixture (40 mL) of absolute CH_3CN:EtOH (*v/v*; 1.7:1) at room temperature, was added dropwise one solution of 1-naphthaldehyde (0.5 g, 3.2 mmol) in dried CH_3CN (10 mL). The solution was stirred at room temperature over 2 h and the solvent was evaporated to dryness. The resulting residue was dissolved in dried EtOH (15 mL) and $NaBH_4$ (1.1 g, 29.5 mmol) was added portion wise. The mixture was stirred at room temperature for 24 h. After that, the mixture was filtered, and the solvent was evaporated under reduced pressure. The residue obtained was extracted with chloroform (3 × 50 mL) and evaporated to dryness obtaining one oil which was dissolved in a mixture of MeOH:EtOH (*v/v*; 1:1) and precipitated with some drops of HCl 37% to give the different naphthalene derivatives:

N^1-(2-aminoethyl)-N^2-(naphtalen-1-ylmethyl)etane-1,2-diamine (Napht-3)

From diethylenetriamine (1.0 g, 9.6 mmol) and 1-naphtaldeyde (0.5 g, 3.2 mmol). Yield: 79% (1.2 g, 4.9 mmol). White solid. mp 203 °C. ^{1}H NMR (400 MHz, DMSO-d_6) δ 9.99–9.35 (m, 3H), 8.18 (t, *J* = 10.1 Hz, 1H), 7.98–7.93 (m, 1H), 7.72–7.46 (m, 2H), 4.67 (s, 1H), 3.44 (s, 4H), 3.11 (s, 4H). ^{13}C NMR (101 MHz, DMSO-d_6) δ 133.7, 131.4, 130.2, 129.3, 129.2, 128.3, 127.4, 126.9, 125.8, 124.2, 47.6, 44.4, 43.7, 43.2, 35.6.

N^1-(2-aminoethyl)-N^2-(2-((2-((naphtalen-1-ylmethyl) amino) ethyl) amino) etyl) etane-1,2-diamine (Napht-5)

From tetraethylenepentamine (1.8 g, 9.6 mmol) and 1-naphtaldeyde (0.5 g, 3.2 mmol). Yield: 11% (0.2 g, 0.7mmol). White solid. mp 310 °C. ^{1}H NMR (400 MHz, DMSO-d_6) δ 10.67–8.64 (m, 2H), 8.50–8.26 (m, 1H), 8.19–7.97 (m, 1H), 7.96–7.44 (m, 2H), 4.83 (d, *J* = 8.0 Hz, 1H), 4.19 (s, 1H), 1.32 (s, 1H). ^{13}C NMR (101 MHz, DMSO-d_6) 133.8, 131.4, 130.2, 129.3, 129.2, 128.3, 127.4, 126.9, 125.8, 124.2, 70.3, 47.7, 44.6, 44.0, 43.4, 36.0, 31.8, 29.5, 29.2.

2.1.3. Synthesis of Phenanthroline Derivatives

2,9-Bis(oxazole-5-yl)-1,10-phenantroline (Phen-1)

The synthesis was performed as previously described [15].

2,9-Dimethy-1,10-phenanthroline-5,6-dione

2,9-Dimethyl-1,10-phenanthroline (2.0 g, 9.6 mmol) was added into a solution of 60% H_2SO_4 (23 mL). To this solution, potassium bromate was added in batches (1.8 g, 11.0 mmol) for 1 h and the mixture was stirred at room temperature for 20 h. After that, the solution

was poured into water (200 mL) and carefully neutralized to pH 7 using a solution of sodium hydroxide 8 M [17]. The precipitate was filtered and washed with water giving a yellow solid with 70% yield (1.6 g, 6.7 mmol); mp 177 °C. ^{1}H NMR (400 MHz, DMSO-d_6) δ (ppm) 8.26 (d, 2H, CH), 7.52 (d, 2H, CH) 2.68 (s, 6H, CH$_3$); ^{13}C NMR (101 MHz, DMSO-d_6) 178.4, 164.7, 152.3, 136.6, 127.2, 125.2, 25.3.

7,10-Dimethylpyrazino[2,3-*f*][1,10]phenanthroline (DPPZ)

2,9-Dimethy-1,10-phenanthroline-5,6-dione (0.6 g, 2.5 mmol) was dissolved in dried EtOH (50 mL) and ethylenediamine was added (0.2 g, 2.9 mmol). The stirred solution was refluxed overnight. After cooling the solution was concentrated to half of the initial volume [18]. The brown solid which formed was filtered obtaining 60% of yield (0.4 g, 1.5 mmol); mp 265–266 °C. ^{1}H NMR (400 MHz, DMSO-d_6): δ (ppm) 9.30 (d, *J* = 8.3 Hz, 2H, CH), 9.10 (s, 1H), 7.80 (d, *J* = 8.3 Hz, 2H, CH), 2.85 (s, 6H, CH$_3$) ^{13}C NMR (101 MHz, DMSO-d_6): δ (ppm) 161.4, 146.6, 145.4, 139.8, 133.2, 124.8, 124.7, 25.5 (CH$_3$).

2,9-Dicarbaldehyde-1,10-phenanthroline (PhenCOH)

SeO$_2$ (4.3 g, 38.4 mmol) was taken in dioxane (100 mL) at 60 °C. To this solution, a small increment of 2,9-dimethyl-1,10-phenanthroline (4.0 g, 19.2 mmol) dissolved in dioxane (35 mL) was added over 2 h and refluxed at 100 °C overnight. The mixture was filtered through celite in a hot condition and dioxane was removed under reduced pressure. The residue was purified by column chromatography using silica gel (0.060–0.200 mm, 60 A) and MeOH:CHCl$_3$ (*v*/*v*; 95:5) solvent mixture [19]. After complete separation, the solution was evaporated under vacuum conditions to give a pale yellow solid with a 50% yield (2.3 g, 9.7 mmol); ^{1}H NMR (400 MHz, CDCl$_3$-d_6): δ (ppm) 10.57 (s, 2H, COH), 8.52 (d, *J* = 8.2 Hz, 2H, CH), 8.39 (d, *J* = 8.1 Hz, 2H, CH), 8.06 (s, 2H, CH). ^{13}C NMR (101 MHz, CDCl$_3$-d_6) δ (ppm) 193.4 (COH), 152.7, 146.0, 138.0, 131.6, 129.1, 120.5.

1,10-Phenanthroline-2,9-dicarboxylic Acid (PhenCOOH)

2,9-Dicarbaldehyde-1,10-phenanthroline (0.6 g, 2.4 mmol) was added into HNO$_3$ (2 mL; 65 wt %). The mixture was refluxed over 6 h, and then the content was poured into cursed ice [19]. The solid was filtered to give a light yellow final product with an 89% yield (0.6 g, 2.2 mmol); ^{1}H NMR (400 MHz, DMSO-d_6): δ (ppm) 8.74 (d, *J* = 8.3 Hz, 2H, CH), 8.42 (d, *J* = 8.2 Hz, 2H, CH), 8.22 (s, 2H, CH). ^{13}C NMR (101 MHz, DMSO-d_6): δ (ppm) 166.7, 148.7, 145.1, 138.7, 131.0, 129.0, 124.0, 40.6, 40.4, 40.2, 40.0, 39.7, 39.5, 39.3.

2,9-Dicarbomethoxy-1,10-phenanthroline (Phen-COOCH$_3$)

1,10-Phenanthroline-2,9-dicarboxylic acid (0.6 g, 2.1 mmol) was suspended in MeOH (150 mL) and conc. H$_2$SO$_4$ (15 mL) was added to this solution. The reaction mixture was refluxed overnight [19]. After that, the mixture was poured into crushed ice and allowed to cool. The precipitate was filtered and was obtained as a light yellow product with a 53% yield (0.3 g, 1.0 mmol); mp 184–186 °C. ^{1}H NMR (400 MHz, CDCl$_3$-d_6): δ (ppm) 8.75 (d, *J* = 8.3 Hz, 2H, CH), 8.43 (d, *J* = 8.2 Hz, 2H, CH), 8.23 (s, 2H, CH), 4.04 (s, 6H, OCH$_3$). ^{13}C NMR (101 MHz, CDCl$_3$-d_6): 166.0, 148.1, 145.5, 138.6, 131.0, 129.0, 124.2, 53.2.

2.1.4. Acridine Derivatives

The synthesis and purification of 10-(5-aminopentyl)-3,6-bis(dimethylamino)acridinium iodide (C$_5$-NH$_2$), and 10-(8-aminooctyl)-3,6-bis(dimethylamino)acridinium iodide (C$_8$-NH$_2$) were performed as described [20].

2.2. Oligonucleotides and Ligands

All the oligonucleotide sequences were obtaining from Eurofins Genomics (Munich, Germany) and Eurogentec (Seraing, Belgium) with HPLC-grade purification. The oligonucleotide sequences were double labelled with fluorescein (FAM) and tetramethylrhodamine (TAMRA) at the 5′ and 3′ ends, respectively. The following oligonucleotide

sequences were used: c-MYC (5′-TGAGGGTGGGTAGGGTGGGTAA-3′), KRAS21 (5′-AGGGCGGTGTGGGAAGAGGGA-3′), 21G (5′-GGGTTAGGGTTAGGGTTAGGG-3′), VEGF (5′-CGGGGCGGGCCGGGGGCGGGGT-3′) pre-MIR150 (5′-GGCCUGGGGGACAGGGAC-CUGGG-3′) and DNA duplex (5′-TATAGCTATA-hexaethyleneglycol-TATAGCTATA-3′). Stock solutions were prepared using Milli-Q water and stored at $-20\ ^\circ$C. The oligonucleotide concentrations were measured at 260 nm with a UV–Vis spectrophotometer (Thermo Scientific™ Evolution 220, Thermo Fisher Scientific, Waltham, MA, USA) using the molar extinction coefficients (ε) provided by the manufacturer. The annealing procedure for FmycT, FkrasT, F21T, FvegfT and FdxT consisted of heating to 95 $^\circ$C for 10 min, followed by cooling in ice for 30 min and for Fpre-MIR150T consisted of heating to 95 $^\circ$C for 10 min, followed by cooling in ice for more than 10 min. Stock solutions of the compounds were prepared as 10 or 5 mM solutions in dimethyl sulfoxide (DMSO) (Thermo Fisher Scientific, Waltham, MA, USA) and their subsequent dilution was done using Milli-Q water.

2.3. In Silico Simulations

In silico studies were performed to estimate some molecular properties of the compounds to be tested in vitro. The structures of the different derivatives tested were drawn in ChemDraw 20.0 software (PerkinElmer, Waltham, MA, USA), and the SMILES notation was obtained for all tested compounds. Molecular weight (MW), n-octanol:water partition coefficient (Log *P*), number of rotatable bonds (n-ROTB), number of hydrogen bond acceptors (n-ON acceptors) and number of hydrogen bond donors (n-OHNH donors) were calculated using pKCSM online software [21] and topological polar surface area (TPSA) was determined by Molinspiration property engine v2018.10 on the Molinspiration online server (www.molinspiration.com, accessed on 15 February 2022).

2.4. Fluorescence Resonance Energy Transfer (FRET) Melting Assays

FRET melting assays were performed in a CFX Connect™ Real-Time PCR Detection System (Bio-Rad, Hercules, CA, USA) equipped with a FAM filter using a 96-well plate. The labelled oligonucleotide sequences were annealed before the experiment as previously described, and the fluorescence intensity was recorded every 1 $^\circ$C between 25 and 95 $^\circ$C with a temperature increment of 1 $^\circ$C min^{-1}. The excitation and detection wavelengths were 492 and 516 nm, respectively. The buffer used in the experiments was 10 mM lithium cacodylate (pH 7.2) supplemented with the necessary amount of KCl and LiCl. The labelled oligonucleotide sequence was used at 0.2 μM and the ligands at 5 or 1 μM final concentration. Each experimental condition was tested in duplicate on two separate assays. The melting temperature was determined from the normalized curves as the mid-transition $T_{1/2}$ temperature (Figure S2).

2.5. Cytotoxicity in Human Cell Lines
2.5.1. Cell Cultures

Non-small human lung adenocarcinoma epithelial cell line (A549) and normal human dermal fibroblasts cell line (NHDF) were purchased at American Type Culture Collection (ATCC), cultured in 75 cm^2 T-flasks and maintained in a humidified atmosphere at 37 $^\circ$C and 5% CO_2. A549 cells were grown with Ham's-F12 medium supplemented with 10% fetal bovine serum (FBS) and 1% streptomycin-penicillin (SP) antibiotic and NHDF with RPMI medium supplemented with 10% FBS, 1% SP antibiotic, 2 mM L-glutamine, 10 mM HEPES and 1 mM sodium pyruvate.

2.5.2. MTT Assay

The in vitro cell proliferation was determined using the 3-(4,5-dimethylthiazol-2-yl)-2,5-diphenyltetrazolium bromide (MTT) (Sigma-Aldrich, St. Louis, MO, USA) assay. The A549 and NHDF cells were plated in 96-well culture plates with density of 1×10^4 cells/mL in the appropriate culture medium. After 48 h of adherence cells were treated with the

different compounds in the study for 72 h. At the end of incubation, the medium was removed and replaced with MTT solution and further incubated at 37 °C for 4 h. Then, the MTT solution was removed, and the resulting formazan crystals were dissolved with 100 μL of DMSO. The absorbance was measured at 570 nm using a microplate reader Biorad Xmark spectrophotometer (Bio-Rad, California, USA). The cytotoxicity was normalized control conditions (untreated cells). Each experiment was performed in quadruplicate in two independent experiments.

3. Results and Discussion

3.1. Chemistry

Several small molecules have been reported in the literature as ligands/drugs for the targeting of G4 structures, including new chemotypes [22]. Among the several classes of ligands, synthetic heterocycles have proven to be a promising scaffold for the design of G4 binders and stabilizers, in particular, fused aromatic compounds.

Herein, we describe the chemical synthesis, full characterization and in vitro evaluation of four different aromatic scaffolds containing oxazole, acridine, naphthalene and phenanthroline moieties. The naphthalene and phenanthroline derivatives were synthesized as shown in Schemes 1 and 2, with low to high yields, i.e., 11–89%, respectively (experimental section). All starting compounds were commercially obtained and most of these derivatives were easily obtained with a high degree of purity, as confirmed for NMR analysis. Naphthalene derivatives (Napht-3 and Napht-5) were synthetized by following a two-step route, previously reported by Clares et al. [16]. Firstly, a condensation between 1-naphtaldehyde and diethylenetriamine and tetraethylenepentamine, followed by in situ reduction in the formed imine with sodium borohydride, gave derivatives Napht-3 and Napht-5 with 79% and 11% yields, respectively (Scheme 1). The phenanthroline derivatives were synthetized using procedures already described (Scheme 2) [17–19]. The synthesis of 7,10-dimethylpyrazino[2,3-*f*][1,10]phenanthroline (DPPZ) was done by initial oxidation of 2,9-dimethyl-1,10-phenanthroline with potassium bromate in sulfuric acid solution, affording 2,9-dimethy-1,l0-phenanthroline-5,6-dione. After that, the dione reacted with ethylenediamine by condensation to give DPPZ with a yield of 60%. The 2,9-dicarbomethoxy-1,10-phenanthroline ($COOCH_3$) was synthetized from the oxidation of 2,9-dimethyl-1,10-phenanthroline to the aldehyde, which was oxidized to a dicarboxylic acid derivative and converted to $PhenCOOCH_3$ by Fisher esterification, in a yield of 53%. The phenyl (ISO-1 and Ter-1), quinoline (Quin-1) and acridine derivatives (C_5NH_2 and C_8NH_2) were synthesized as previously described [15,20].

R$_1$ = diethylenetriamine; η = 79%

tetraethylenepentamine; η = 11%
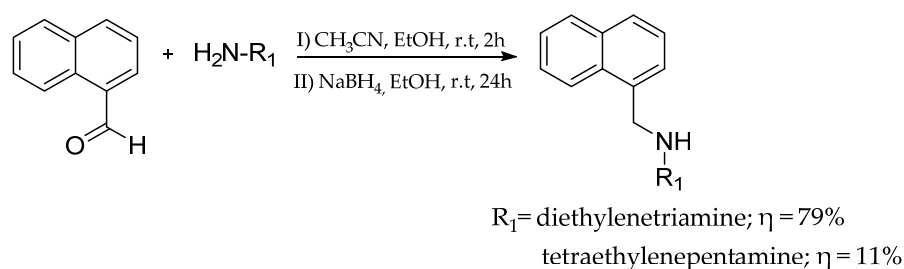
Scheme 1. Chemical synthesis of naphthalene derivatives.
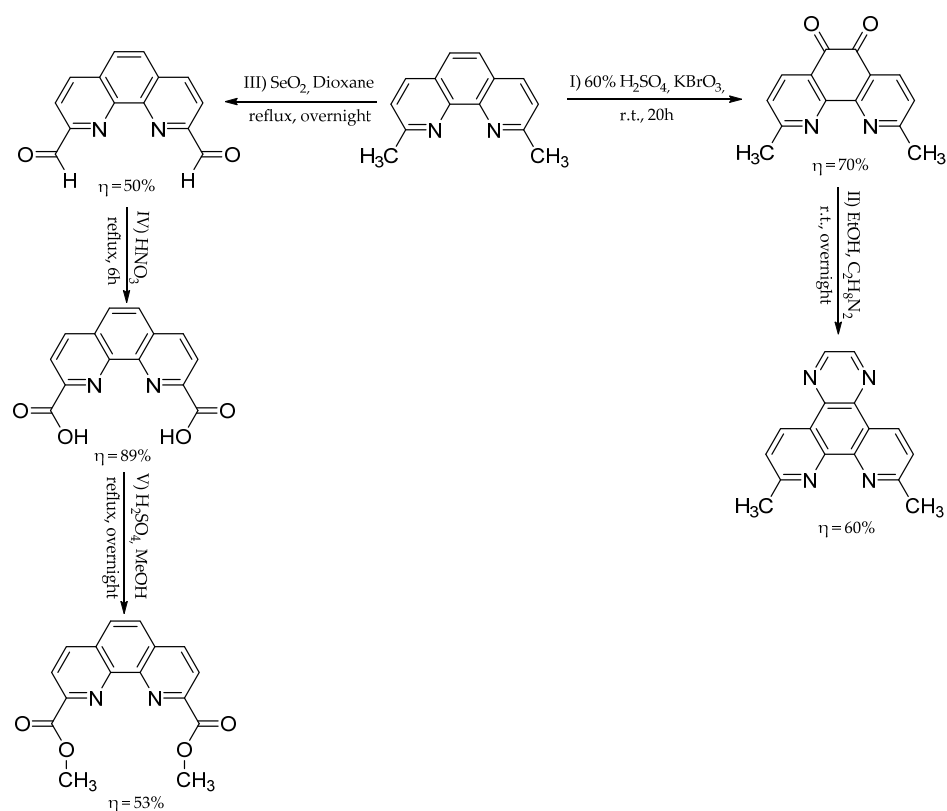
Scheme 2. Chemical synthesis of phenanthroline derivatives.

3.2. In Silico Studies

Taking into account that G4 ligands present poor drug-like properties, a computational study using Lipinski's rule and Veber's parameters was performed to predict in vitro permeation and oral absorption [23,24]. The in silico parameters are presented in Table 1. All tested ligands presented MW (210.236–395.615), Log *P* (0.657–4.093), n-ON acceptors (3–6) and n-OHNH donors (0–5), in the range defined by Lipinski's rule [23]. The n-ROTB between 2 and 13 and TPSA from 38.92 to 181.68, revealed that most of the tested scaffolds comply with Veber's parameters (n-ROTB < 10 and TPSA < 10 Å^2) [24]. None of the tested ligands violated Lipinski´s rule of five, indicating that they have favorable properties that achieve the criteria of drug-likeness.

Table 1. In silico molecular descriptors of in vitro evaluated compounds [a].

Ligand	TPSA	MW	Log *P*	n-ROTB	n-ON Acceptors	n-OHNH Donors	Lipinski's Violations [b]
Ter-1	181.68	212.208	2.997	2	4	0	0
ISO-1	52.06	212.208	2.997	2	4	0	0
Quin-1	38.92	210.236	3.198	1	3	0	0
Napht-3	50.08	243.354	1.48	7	3	3	0
Napht-5	74.13	329.492	0.657	13	5	5	0
Phen-1	77.85	314.304	4.093	2	6	0	0
DPPZ	51.57	260.3	3.343	0	4	0	0
PhenCOOCH$_3$	78.39	296.282	2.356	2	6	0	0
C$_8$NH$_2$	35.50	395.615	2.3372	10	3	1	0
C$_5$NH$_2$	35.50	353.534	1.1669	7	3	1	0

[a] TPSA, topological polar surface area (Å^2); molecular weight (g/mol); Log *P* (n-octanol:water partition coefficient); n-ROTB (number of rotatable bonds); n-ON acceptors (number of hydrogen bond acceptors); n-OHNH donors (number of hydrogen bond donors). [b] Lipinski rule of five: MW < 500 Da; Log *P* ≤ 5; n-OHNH acceptors ≤ 10; n-OHNH donors ≤ 5. A maximum of 1 violation is generally permitted.

3.3. FRET Melting Studies

The ability of the scaffolds to bind and stabilize G4 structures was evaluated by a high-throughput FRET melting assay [25]. This method is commonly used for first screening of G4 binding and stabilization efficiency of a small molecule [19]. The scaffolds were tested against four G4 DNA sequences (c-MYC, KRAS21 and VEGF promoters, and 21G human telomeric repeats) one G4 RNA (pre-MIR150) [26] and a double-stranded DNA control. The ligands were screened at 5 μM, except acridine derivatives, which were tested at 1 μM. The melting temperatures are summarized in Table 2.

Table 2. The thermal stabilization induced by different scaffolds measured by FRET-melting experiments.

Ligand Concentration	Ligand	ΔT_m (°C)					
		FmycT	F21T	FkrasT	FvegfT	Fpre-MIR150T	FdxT
5 μM	Ter-1	0.0 ± 0.2	0.0 ± 0.0	0.0 ± 1.9	0.0 ± 1.6	0.0 ± 0.5	0.0 ± 0.1
	ISO-1	0.0 ± 0.3	0.1 ± 0.0	0.0 ± 1.0	0.5 ± 1.2	0.0 ± 0.0	0.0 ± 0.3
	Quin-1	0.0 ± 1.0	0.2 ± 0.5	0.0 ± 0.9	0.0 ± 2.0	0.0 ± 0.2	0.0 ± 0.0
	Napht-3	0.0 ± 0.1	0.8 ± 0.3	2.0 ± 1.0	0.6 ± 2.1	0.0 ± 0.3	0.0 ± 0.4
	Napht-5	0.0 ± 0.2	0.8 ± 0.1	0.1 ± 1.0	0.0 ± 1.9	0.0 ± 0.3	0.0 ± 0.2
	Phen-1	0.0 ± 0.1	2.5 ± 0.1	0.3 ± 0.6	0.0 ± 2.0	0.0 ± 0.1	0.0 ± 0.2
	DPPZ	0.6 ± 0.3	0.4 ± 0.1	0.6 ± 0.2	0.0 ± 1.4	0.0 ± 0.1	0.0 ± 0.2
	PhenCOOCH$_3$	0.6 ± 0.8	3.4 ± 0.2	3.4 ± 1.8	0.0 ± 2.0	0.0 ± 0.1	0.0 ± 0.3
1 μM	C$_8$NH$_2$	17.4 ± 0.4	26.8 ± 0.3	7.2 ± 0.4	4.5 ± 0.5	4.6 ± 0.0	0.1 ± 0.1
	C$_5$NH$_2$	16.3 ± 0.2	15.6 ± 0.2	18.0 ± 2.6	2.5 ± 0.9	0.9 ± 1.3	0.3 ± 0.2

ΔT_m represents the difference in melting temperature [$\Delta T_m = T_m$ (G4 sequence + ligand) $- T_m$ (G4 sequence)]. The buffer used was 10 mM lithium cacodylate, pH 7.2 with addition of extra concentrations of KCl and LiCl. The T_m values for the DNAs are 65.3 ± 0.1 °C [c-MYC promoter DNA in 10 mM KCl and 90 mM LiCl], 52.1 ± 0.2 °C [21G telomeric DNA in 10 mM KCl and 90 mM LiCl], 41.4 ± 2.1 °C [KRAS promoter DNA in 10 mM KCl and 90 mM LiCl], 66.9 ± 2.0 °C [VEGF promoter DNA in 1 mM KCl and 99 mM LiCl], for the RNA is 68.5 ± 0.2 °C [pre-MIR150 in 1 mM KCl and 99 mM LiCl] and 65.3 ± 0.0 °C [duplex DNA in 100 mM KCl]. Each experimental condition was done in duplicate, and the values correspond to the average of two independent experiments with the estimated standard deviation. Negative ΔT_m values are reported as zero.

Overall, FRET-melting data showed that screened scaffolds are poor G4 stabilizers, with the notable exception of two acridine precursors, C$_8$NH$_2$ and C$_5$NH$_2$. This evidence suggests that the alkylamino chain is also important for G4 binding and stabilization beyond the aromatic ring. C$_8$NH$_2$ proved to be the most effective binder for all G4 sequences (ΔT_m = 17.4 °C for FmycT, 26.8 °C for F21T, 7.2 °C for FkrasT, 4.5 °C for FvegfT, and 4.6 °C for Fpre-MIR150T at 1 μM concentration), followed by C$_5$NH$_2$ (ΔT_m = 16.3 °C for FmycT, 15.6 °C for F21T, 18.0 °C for FkrasT, 2.5 °C for FvegfT, and 0.9 °C for Fpre-MIR150T at 1 μM concentration). The FRET-melting studies corroborate the other series of acridine derivatives, in which the nature of the acridine scaffold and the alkylamide chain influence the G4 stabilization. Previous studies have shown that the acridine moiety interacts with the G4 surface by end stacking interactions and the alkylamide interacts by groove binding [27]. In addition, acridine derivatives have stronger G4 stabilizing efficiency on pre-miRNA structure [28].

The phenyl and quinoline scaffolds displayed null stabilization of the DNA/RNA G4 structures studied, when compared with phenanthroline derivatives. The phenanthroline analogue Phen-2, described previously, which has a π system extension, showed an increase in melting temperature of FmycT and F21T, when compared with its precursor, Phen-1. Compound Phen-1 exhibited a minimal increase in T_m of 2.5 °C to F21T and no stabilization of FmycT even at 5 μM, while the Phen-2 showed a moderate increase in T_m of 8.6 °C for F21T and 11.3 °C for FmycT at the same concentration [15]. The functionalization with ester group in the phenanthroline moiety, when compared with oxazole functionalization, improved the G4 binding capacity against F21T and FkrasT sequences. On the contrary, the introduction of an additional pyrazine ring in phenanthroline moiety reduced stabi-

lization effect on all G4s. Compounds containing naphthalene scaffolds presented poor G4 stabilization, which was slightly better for FkrasT, in the case of derivatives containing a short polyamine chain linked directly to the ring (Napht-3). All tested scaffolds exhibited negligible stabilization for FdxT (Table 2).

3.4. Cytotoxicity Assay

The scaffold's effect on cell viability was evaluated by an MTT assay, using A549 lung cancer and NHDF healthy cell lines. The results of IC_{50} are presented in Table 3. Overall, the scaffolds were found to be much more active on the cancer cell line. The acridine precursors showed a high potency against the A549 cell line, with IC_{50} values of 1.3 μM (C_8NH_2) and 3.6 μM (C_5NH_2). Most relevantly, C_5NH_2 shows an IC_{50} of 17.8 μM in normal human fibroblasts, indicating a good selectivity for its cellular growth inhibitory activity in human cancer cells over human normal cells. The anticancer activity of C_8NH_2 is consistent with that previously reported for PC-3 (prostate adenocarcinoma) and PNT1A (normal human prostate cell line) [28]. These results can be correlated with the FRET-melting results, which may indicate that the cytotoxicity effect of the acridine ligands can be related to G4 binding ability. On the contrary, the phenanthroline scaffold containing a pyrazine ring (DPPZ) showed lower IC_{50} values in both cell lines (IC_{50} of 0.4 μM and 0.2 μM for cancer and normal cell line, respectively), suggesting lower cellular selectivity. Most probably, this effect is not mediated by G4 binding, since DPPZ showed weak G4 stabilizer capacity in FRET-melting experiments. The phenanthroline derivative containing an oxazole ring (Phen-1) presented low and no-selective cytotoxicity effect in cancer (IC_{50} = 22.1 μM) and healthy (IC_{50} = 20.4 μM) cell lines. Conversely, the introduction of an ester group in the phenanthroline scaffold conferred potency against A549 cells (IC_{50} = 6.4 μM) and a weak inhibitory effect on healthy cells (IC_{50} = 37.0 μM). Therefore, PhenCOOCH$_3$ can be a promising candidate for further cellular studies. Similarly, phenyl (Ter-1 and ISO-1) derivatives were shown to be promising anticancer candidates, particularly Ter-1, with a pronounced cytotoxicity effect in cancer cells (IC_{50} = 1.9 μM) and weak toxicity in healthy cells (IC_{50} = 34.0 μM). These results suggest that the 1,4 disubstituted phenyl ring confers higher anticancer activity, when compared with the 1,3 disubstituted congener (ISO-1; with an IC_{50} value of 9.8 and 32.0 μM for cancer and healthy cells lines, respectively). The Quinoline derivative also presents selectivity and cytotoxicity effects (IC_{50} = 9.0 μM) in cancer cells. Naphthalene scaffolds exhibited a low inhibitory effect on the cancer cell line, but Napht-3 presented low IC_{50} on the fibroblast cell line (NHDF). This trend can be related with the size of the polyamine chain, since Napht-3 has a short polyamine chain and is more toxic in normal cells (IC_{50} = 5.3 μM) than the derivative containing the pentamine chain (Napht-5; IC_{50} = 24.1 μM). For cancer cells, Napht-5 is more potent (IC_{50} = 12.5 μM) than Napht-3 (IC_{50} = 19.4 μM).

Table 3. IC_{50} [a] values induced by different scaffolds in A549 and NHDF cell lines.

Ligand	IC_{50} (μM)		Selectivity Factor
	A549	**NHDF**	
Ter-1	1.9	34.0	17.9
ISO-1	9.8	32.0	3.3
Quin-1	9.0	32.6	3.6
Napht-3	19.4	5.3	0.3
Napht-5	12.1	24.1	2.0
Phen-1	22.0	20.7	0.9
DPPZ	0.40	0.21	0.5
PhenCOOCH$_3$	6.4	37.0	5.8
C_8NH_2	1.3	3.8	2.9
C_5NH_2	3.6	17.8	4.9

[a] IC_{50} values were determined in two separate experiments independently with a 95% confidence interval.

4. Conclusions

Different scaffolds of phenyl, quinoline, naphthalene, phenanthroline and acridine types have been investigated for their G4 binding potential. Four of these scaffolds (Napht-3, Napht-5, DPPZ and PhenCOOCH$_3$) were synthetized and screened for the first time against a G4 structure. Concerning their synthesis, the derivatives were obtained with moderate to good yields. The FRET-melting experiments showed that the acridine compounds are the most promising scaffolds and, most importantly, C$_8$NH$_2$ can discriminate among different G4 structures. Overall, the different molecules did not present a high pronounced toxic effect in normal cell lines, in contrast to cancers cells. Additionally, these scaffolds hit the drug-like criteria. This study could lead to the identification of G4-interactive molecules, deserving further optimization of their structures towards the development of drug candidates.

References

1. Figueiredo, J.; Santos, T.; Miranda, A.; Alexandre, D.; Teixeira, B.; Simões, P.; Lopes-Nunes, J.; Cruz, C. Ligands as Stabilizers of G-Quadruplexes in Non-Coding RNAs. *Molecules* **2021**, *26*, 6164. [CrossRef] [PubMed]
2. Abiri, A.; Lavigne, M.; Rezaei, M.; Nikzad, S.; Zare, P.; Mergny, J.-L.; Rahimi, H.-R. Unlocking G-Quadruplexes as Antiviral Targets. *Pharmacol. Rev.* **2021**, *73*, 897–923. [CrossRef] [PubMed]
3. Sun, D.; Thompson, B.; Cathers, B.E.; Salazar, M.; Kerwin, S.M.; Trent, J.O.; Jenkins, T.C.; Neidle, S.; Hurley, L.H. Inhibition of human telomerase by a G-Quadruplex-Interactive compound. *J. Med. Chem.* **1997**, *40*, 2113–2116. [CrossRef] [PubMed]
4. Wheelhouse, R.T.; Sun, D.; Han, H.; Han, F.X.; Hurley, L.H. Cationic porphyrins as telomerase inhibitors: The interaction of tetra-(*N*-methyl-4-pyridyl)porphine with quadruplex DNA. *J. Am. Chem. Soc.* **1998**, *120*, 3261–3262. [CrossRef]
5. Guliaev, A.B.; Leontis, N.B. Cationic 5,10,15,20-Tetrakis(*N*-methylpyridinium-4-yl)porphyrin Fully Intercalates at 5′-CG-3′ Steps of Duplex DNA in Solution. *Biochemistry* **1999**, *38*, 15425–15437. [CrossRef] [PubMed]
6. Lee, Y.-A.; Kim, J.-O.; Cho, T.-S.; Song, R.; Kim, S.K. Binding of meso-Tetrakis(*N*-methylpyridium-4-yl)porphyrin to Triplex Oligonucleotides: Evidence for the Porphyrin Stacking in the Major Groove. *J. Am. Chem. Soc.* **2003**, *125*, 8106–8107. [CrossRef]
7. Kim, M.Y.; Vankayalapati, H.; Shin-Ya, K.; Wierzba, K.; Hurley, L.H. Telomestatin, a potent telomerase inhibitor that interacts quite specifically with the human telomeric intramolecular G-quadruplex. *J. Am. Chem. Soc.* **2002**, *124*, 2098–2099. [CrossRef]

8.   Franceschin, M.; Rossetti, L.; D'Ambrosio, A.; Schirripa, S.; Bianco, A.; Ortaggi, G.; Savino, M.; Schultes, C.; Neidle, S. Natural and synthetic G-quadruplex interactive berberine derivatives. *Bioorg. Med. Chem. Lett.* **2006**, *16*, 1707–1711. [CrossRef]

9.   Chambers, V.S.; Marsico, G.; Boutell, J.M.; Di Antonio, M.; Smith, G.P.; Balasubramanian, S. High-throughput sequencing of DNA G-quadruplex structures in the human genome. *Nat. Biotechnol.* **2015**, *33*, 877–881. [CrossRef]

10.   Xu, H.; Di Antonio, M.; McKinney, S.; Mathew, V.; Ho, B.; O'Neil, N.J.; Dos Santos, N.; Silvester, J.; Wei, V.; Garcia, J.; et al. CX-5461 is a DNA G-quadruplex stabilizer with selective lethality in BRCA1/2 deficient tumours. *Nat. Commun.* **2017**, *8*, 14432. [CrossRef]

11.   Drygin, D.; Lin, A.; Bliesath, J.; Ho, C.B.; O'Brien, S.E.; Proffitt, C.; Omori, M.; Haddach, M.; Schwaebe, M.K.; Siddiqui-Jain, A.; et al. Targeting RNA Polymerase I with an Oral Small Molecule CX-5461 Inhibits Ribosomal RNA Synthesis and Solid Tumor Growth. *Cancer Res.* **2011**, *71*, 1418–1430. [CrossRef] [PubMed]

12.   Das, R.; Chevret, E.; Desplat, V.; Rubio, S.; Mergny, J.-L.; Guillon, J. Design, Synthesis and Biological Evaluation of New Substituted Diquinolinyl-Pyridine Ligands as Anticancer Agents by Targeting G-Quadruplex. *Molecules* **2017**, *23*, 81. [CrossRef] [PubMed]

13.   Hamon, F.; Largy, E.; Guédin-Beaurepaire, A.; Rouchon-Dagois, M.; Sidibe, A.; Monchaud, D.; Mergny, J.-L.; Riou, J.-F.; Nguyen, C.-H.; Teulade-Fichou, M.-P. An Acyclic Oligoheteroaryle That Discriminates Strongly between Diverse G-Quadruplex Topologies. *Angew. Chem. Int. Ed.* **2011**, *50*, 8745–8749. [CrossRef]

14.   De Rache, A.; Mergny, J.-L. Assessment of selectivity of G-quadruplex ligands via an optimised FRET melting assay. *Biochimie* **2015**, *115*, 194–202. [CrossRef] [PubMed]

15.   Medeiros-Silva, J.; Guédin, A.; Salgado, G.F.; Mergny, J.-L.; Queiroz, J.A.; Cabrita, E.J.; Cruz, C. Phenanthroline-bis-oxazole ligands for binding and stabilization of G-quadruplexes. *Biochim. Biophys. Acta Gen. Subj.* **2017**, *1861*, 1281–1292. [CrossRef]

16.   Clares, M.P.; Aguilar, J.; Aucejo, R.; Lodeiro, C.; Albelda, M.T.; Pina, F.; Lima, J.C.; Parola, A.J.; Pina, J.; Seixas De Melo, J.; et al. Synthesis and H^+, Cu^{2+}, and Zn^{2+} Coordination Behavior of a Bis(fluorophoric) Bibrachial Lariat Aza-Crown. *Inorg. Chem.* **2004**, *43*, 6114–6122. [CrossRef]

17.   Zheng, R.H.; Guo, H.C.; Jiang, H.J.; Xu, K.H.; Liu, B.B.; Sun, W.L.; Shen, Z.Q. A new and convenient synthesis of phendiones oxidated by KBrO3/H2SO4 at room temperature. *Chin. Chem. Lett.* **2010**, *21*, 1270–1272. [CrossRef]

18.   Garas, A.M.S.; Vagg, R.S. Synthesis of some novel derivatives of 1,10-phenanthroline. *J. Heterocycl. Chem.* **2000**, *37*, 151–158. [CrossRef]

19.   R, S.K.; Kumar, S.K.A.; Vijayakrishna, K.; Sivaramakrishna, A.; Brahmmananda Rao, C.V.S.; Sivaraman, N.; Sahoo, S.K. Development of the Smartphone-Assisted Colorimetric Detection of Thorium by Using New Schiff's Base and Its Applications to Real Time Samples. *Inorg. Chem.* **2018**, *57*, 15270–15279. [CrossRef]

20.   Pereira, E.; do Quental, L.; Palma, E.; Oliveira, M.C.; Mendes, F.; Raposinho, P.; Correia, I.; Lavrado, J.; Di Maria, S.; Belchior, A.; et al. Evaluation of Acridine Orange Derivatives as DNA-Targeted Radiopharmaceuticals for Auger Therapy: Influence of the Radionuclide and Distance to DNA. *Sci. Rep.* **2017**, *7*, 42544. [CrossRef]

21.   Pires, D.E.V.; Blundell, T.L.; Ascher, D.B. pkCSM: Predicting small-molecule pharmacokinetic and toxicity properties using graph-based signatures. *J. Med. Chem.* **2015**, *58*, 4066–4072. [CrossRef] [PubMed]

22.   Li, Q.; Xiang, J.-F.; Yang, Q.-F.; Sun, H.-X.; Guan, A.-J.; Tang, Y.-L. G4LDB: A database for discovering and studying G-quadruplex ligands. *Nucleic Acids Res.* **2013**, *41*, D1115–D1123. [CrossRef] [PubMed]

23.   Lipinski, C.A. Drug-like properties and the causes of poor solubility and poor permeability. *J. Pharmacol. Toxicol. Methods* **2000**, *44*, 235–249. [CrossRef]

24.   Veber, D.F.; Johnson, S.R.; Cheng, H.Y.; Smith, B.R.; Ward, K.W.; Kopple, K.D. Molecular properties that influence the oral bioavailability of drug candidates. *J. Med. Chem.* **2002**, *45*, 2615–2623. [CrossRef] [PubMed]

25.   De Cian, A.; Guittat, L.; Kaiser, M.; Sacca, B.; Amrane, S.; Bourdoncle, A.; Alberti, P.; Teulade-Fichou, M.; Lacroix, L.; Mergny, J. Fluorescence-based melting assays for studying quadruplex ligands. *Methods* **2007**, *42*, 183–195. [CrossRef] [PubMed]

26.   Figueiredo, J.; Miranda, A.; Lopes-Nunes, J.; Carvalho, J.; Alexandre, D.; Valente, S.; Mergny, J.-L.; Cruz, C. Targeting nucleolin by RNA G-quadruplex-forming motif. *Biochem. Pharmacol.* **2021**, *189*, 114418. [CrossRef]

27.   Carvalho, J.; Pereira, E.; Marquevielle, J.; Campello, M.P.C.; Mergny, J.-L.; Paulo, A.; Salgado, G.F.; Queiroz, J.A.; Cruz, C. Fluorescent light-up acridine orange derivatives bind and stabilize KRAS-22RT G-quadruplex. *Biochimie* **2018**, *144*, 144–152. [CrossRef]

28.   Santos, T.; Miranda, A.; Campello, M.P.C.; Paulo, A.; Salgado, G.; Cabrita, E.J.; Cruz, C. Recognition of nucleolin through interaction with RNA G-quadruplex. *Biochem. Pharmacol.* **2021**, *189*, 114208. [CrossRef]